ACS APPLIED MATERIALS & INTERFACES

Letter

www.acsami.org

Electroresponsive Aqueous Silk Protein As "Smart" Mechanical Damping Fluid

Rod R. Jose, Roberto Elia, Lee W. Tien, and David L. Kaplan*

Department of Biomedical Engineering, Tufts University Science and Technology Center, 4 Colby Street, Medford, Massachusetts 02155, United States

Supporting Information

ABSTRACT: Here we demonstrate the effectiveness of an electroresponsive aqueous silk protein polymer as a smart mechanical damping fluid. The aqueous polymer solution is liquid under ambient conditions, but is reversibly converted into a gel once subjected to an electric current, thereby increasing or decreasing in viscosity. This nontoxic, biodegradable, reversible, edible fluid also bonds to device surfaces and is demonstrated to reduce friction and provide striking wear protection. The friction and mechanical damping coefficients are shown to modulate with electric field exposure time and/or intensity. Damping coefficient can be modulated electrically, and then preserved without continued power for longer time scales than conventional "smart" fluid dampers.

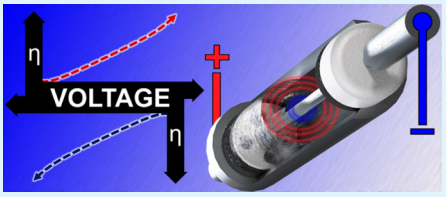

KEYWORDS: *damper, viscous damping, dashpot, friction, electrogelation, electrorheology, silk*

INTRODUCTION

Systems that provide mechanical damping are ubiquitous in nearly all areas of mechanical devices, structures, and robotics. Damping systems function in aspects of padding and hydraulics that provide control, safety, and ergonomics to equipment and human users. "Smart" systems that have the ability to actively modulate damping coefficients in real-time are now considered the modern ideal, and allow for better control and reduced wear.

Dashpot dampers resist motion and absorb energy via viscous friction. They are capable of handling the extreme forces generated by automobiles and aircraft catapults but simpler versions are scaled down for use in humanoid robots and small consumer electronics. Advanced dashpots can be used in conjunction with modern electrorheological (ER) or magnetorheological (MR) fluids in order to actively modulate resistance. ER and MR fluids are modulated in direct response to the intensity of the electric or magnetic field.[1,2] Decreases in viscosity automatically occur with a decrease in field intensity until the magnitude approaches zero, at which point ER and MR fluids return to a liquid state.[1−3]

ER fluids can operate at low current (0.01 to 1 A) but require a nominal voltage of 1000 V to 5000 V, whereas many MR fluids can operate at 5 to 24 V but require a much higher current (1−2 A).[1,2,4] As a result, operating power of typical ER and MR damping devices is 10 to 100 W. These power requirements necessitate more cumbersome form factors and may impose dangers which prohibit use in applications such as human prosthetics. Modern design of these systems has trended toward simplifying the number of required mechanical components in conjunction with elimination of toxic fluid constituents and reduction of operational power requirements. Low power damping systems with a smaller form factors and no risk of toxic discharge or leaching would be useful in a variety of applications.

Here we demonstrate the development and performance of a low-power, physiologically, and environmentally safe active viscous damping system. Silk polymers have been studied for a broad range of biomedical and engineering applications because of the distinctive properties they possess in the crystallized state.[5−7] More recently, the unique chemical properties of uncrystallized aqueous silk solutions have been identified.[8−10]

This system introduces a nontoxic, biodegradable, and edible silk protein fluid that is electroresponsive. The silk fluid, used within this system, is capable of reversibly increasing or decreasing viscous drag, through a process referred to as electrogelation.[8,11,12] The electroresponsive shear yield stress of the silk fluid can be compared to nontoxic ER fluids, and can also be continuously or discretely adjusted.[13] In comparison, the silk electrogelatable fluid operates at lower voltage (5 to 15 V) and lower current (0.01 A), requiring a significantly lower operating power of 0.05−0.15 W. These properties facilitate the development of safer and more mobile damping devices.

EXPIMENTAL DETAILS

Bombyx mori silk cocoons were boiled in 0.02 M aqueous Na_2CO_3 for 10 min in order to isolate the silk fibroin protein for production of 5−7% (w/v) silk solutions following published procedures.[14] Plastic viscosities (n = 3) were measured using a cone and plate viscometer following standard procedures and were reported as the slope of the shear stress/shear rate line above the corresponding yield point. The simplest design of our device is similar to a standard dashpot damper. The main housing acts as the working cylinder (WC), which contains

Received: March 3, 2014
Accepted: April 21, 2014
Published: April 21, 2014

   dx.doi.org/10.1021/am501242w | ACS Appl. Mater. Interfaces 2014, 6, 6212−6216

the components and fluid. The piston rod (PR) terminated with three 1 mm thick Teflon orifice plates, which formed the damper piston. The orifice plates contained four large orifices and a 1.5 mm clearance from the cylinder wall, which left 45% of the cross-sectional area free for fluid travel. Electrode leads were mounted to the aluminum WC and stainless steel PR in order to induce reversible viscosity changes within the device via electrogelation. The positive or negative charge was applied at the PR mounting, while the opposite charge was applied at the WC. Electrogelation was conducted following published procedures using a current of 0.01 A at 5 or 15 V.[8]

Electrogelation was induced continuously or discretely for 30, 60, 90, or 120 s. For discrete gelation, the fluid was subjected to electrogelation for each time period, and then the electrical field was disabled thereby halting the gelation process before mechanical testing. After 120 s of electrogelation, the field was reversed for 30 s. Mechanical testing was conducted throughout ten stroke cycles without applied current. Dunnett's multiple comparison post-test was used to compare the damping of each stroke ($n = 40$) using stroke 2 as the control in order to account for the initial sloughing of gel. Alternatively, the electrogelation was applied continuously during 450 actively reciprocating stroke cycles during which the piston rod traveled 10 mm at a velocity of 1 mm per second per cycle. Solution was brought to the damping plateau then charge was reversed and damping was reduced to the minimal capability after this preconditioning step. Damping coefficient was calculated as the quotient of the force in Newtons caused by viscous drag divided by the velocity of the piston in meters per second. The damping coefficient was given in units of newton-seconds per meter. Fold damping enhancement was normalized to the minimal damping capability. The change in mean damping coefficients between strokes ($n = 5$) during gelation was reported. Continuous tests were compared using standard unpaired t tests. In order to quantify reduction of friction by the electrogelated fluid, three stainless steel plates were subjected to pull-out tests and compared to uncoated plates. Electrogelation was induced for 0, 15, or 60 s using a current of 0.01 A at 15 V. Each plate was mounted between a knurled clamping area of 15 × 25 mm using a normal force of 1.5 kN. Friction force ($n = 3$) was reported as one-half of the peak force required to initiate linear motion, to account for the two surface interfaces. Stainless steel plates ($n = 3$) receiving the same electrogelation treatments were also subjected to surface marring via brass bristles held at an interfacial pressure of 175 kPa for 350 rotational cycles. For all values, variability is reported as standard deviation and depicted with error bars. Asterisks centered over the error bar indicate the relative level of the p-value ($*p < 0.05$, $**p < 0.01$, $***p < 0.001$).

RESULTS AND DISCUSSION

The silk polymer fluid is liquid under ambient conditions; however it is converted into a gel via electrogelation once subjected to an electric field.[8,11] Here we design an electrogelation system capable of exploiting this phenomenon as a "smart" fluid for the function of mechanical damping. To validate the ability of our electrogelation system to modulate damping coefficient as a result of viscous drag, a simple linear dashpot damper was designed with conductive mountings and a large piston orifice area (Figure 1). The conductive mountings are utilized to initiate electrogelation of the silk damping fluid, and the large orifice area is designed to minimize the possibility of erroneous plate-to-wall contact friction, thereby emphasizing resistance due to viscous drag.

During the electrogelation process of the fluid, the gel originates at the positive electrode and progresses outward with time of exposure.[8] The induced electric field acts on the negatively charged amino acids, causing the migration of silk protein toward the cathode. At the cathode, production of hydrogen ions results in a localized drop of solution pH. Once the pI of silk (~4.2) is reached, the silk undergoes folding

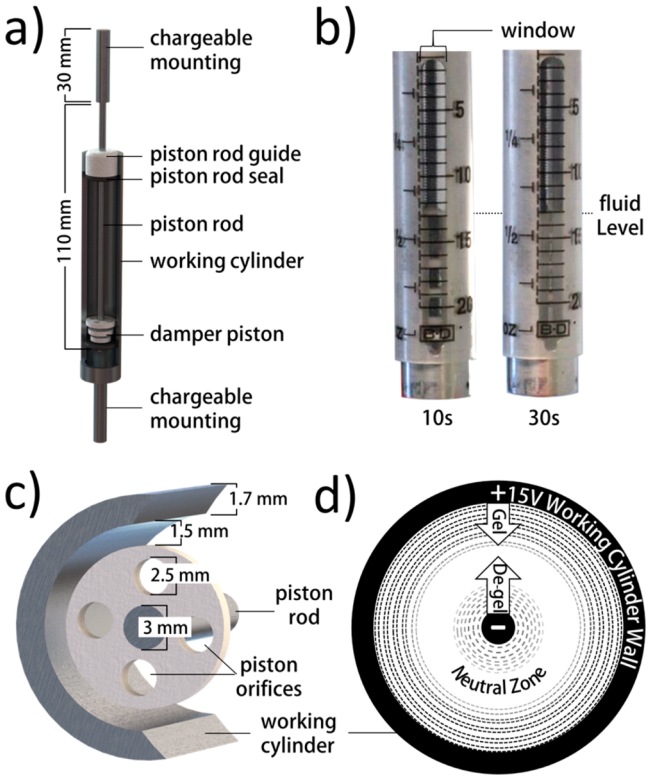

Figure 1. (a) Schematic of prototype components. The working cylinder has been partially cut away to expose internal components. The working cylinder is filled with fluid above and below the piston. (b) Propagation of gelation after 10 or 30 s of exposure to an electric current within the prototype. (c) Schematic cross-section which details one of the three 1 mm thick Teflon orifice places, which form the damper piston. (d) Cross-section that describes the progression of gelation or degelation of the fluid in response to a given configuration of charged components.

interactions, which lead to the formation of micelles that aggregate to form reversible hydrogels.[8] The time of exposure and magnitude of the electric potential can be modulated to affect fluid viscosity (Table 1).

As viscosity is dependent on electrogelation time and intensity, the viscous drag damping coefficient correlates as expected. Damping coefficient can be continuously enhanced severalfold within a working damper with uninterrupted electrogelation of the fluid using a 5 or 15 V potential at 0.01A (Figure 2). The transformation of the fluid into a gel is driven by a localized drop in pH, and conversely exposure to a reversed current leads to a localized increase of pH around the hydrogel.[12] Thus, reversal of the charge reverses the gelation via deprotonation of charged amino acids and subsequent dissociation of the micellular network.

In general, applying higher voltage results in an increase of the damping coefficient by more than one order magnitude and significantly increases the minimal damping coefficient capable of being reached after field reversal (Figure 2a). When the potential is reduced from 15 to 5 V, the time to maximum damping plateau increases nearly 3-fold but results in faster damping reduction when the field is reversed.

Electrogelation is more extensive and reversibility is more consistent with increasing surface area of components, as was evident when positive charge is applied at the working cylinder (Figure 2a). Upon charge reversal, the larger WC surface area

Table 1. Effect of Electric Field Exposure Time at 15 V on Viscosity and Lubrication Performance

time[a] (s)	η^b (cP)	τ^{oc} (Pa)	c^d (Ns m^{-1})	$f_{friction}{}^e$ (N)	$\mu_s{}^f$	R_a AWP[g] (nm)
no fluid	NA	NA	NA	402 ± 76	0.27 ± 0.05	152 ± 22
0	4.8 ± 1.7	0.1 ± 0.05	0.0057 ± 0.0008	320 ± 22	0.21 ± 0.01	47 ± 44
15	−1127 ± 152	48 ± 8	0.56 ± 0.02	252 ± 32	0.17 ± 0.02	38 ± 9
60	−2389 ± 296	169 ± 24	2.61 ± 0.19	204 ± 16	0.14 ± 0.01	4 ± 32

[a]Time of fluid exposure to electric field with cylinder wall at 15 V. [b]Plastic viscosity. [c]Yield stress. [d]Absolute value of damping coefficient. [e]Friction force between knurled clamps under a normal force of 1.5 kN. [f]Static coefficient of friction. [g]Antiwear property measured as the increase in average surface roughness after marring. Initial surface roughness was 200 ± 6 nm.

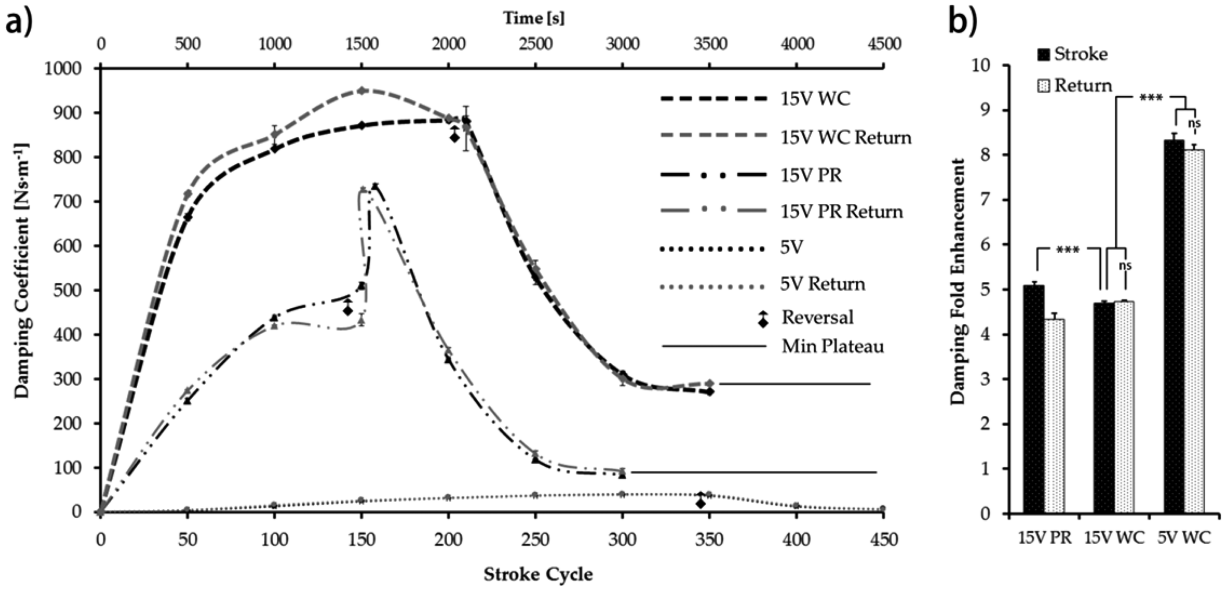

Figure 2. As the damper functions for reciprocal motion, the complete stroke cycle includes the initial actuation stroke (black) through the silk damping fluid, and also the subsequent reverse motion (gray) as the piston returns to the original position. Initial stroke is shown paired with the return stroke in order to demonstrate damping ability is preserved after the initial stroke. (a) Comparison of stroke and return damping coefficients (n = 5) during continuous electrogelation, then after charge reversal. Compares effect of gel propagation from the piston rod (PR) or working cylinder (WC). (b) Fold damping enhancement (n = 5) relative to the subsequent minimal plateau (t test ***p < 0.001).

produces a degelation rate which is greater than the gelation rate occurring at the PR, however the PR-induced gelation is sufficient to produce a minimal damping plateau. This minimal plateau is supplemented by gelated silk aggregates which become suspended in the neutral zone between the WC wall and the PR, because of sloughing after physical strokes (Figure 1d). In contrast, when the positive charge is initially applied to the PR, reversal of the field temporarily induces a 50% increase in damping before a steady decline. This is due to the dependence of opposing gelation and degelation rates on surface area.

Because of the dependency of absolute measured values on device geometry, comparison of the ratios of ultimate resistive force to the corresponding minimal plateaus may better describe the potential of this strategy. The ratio of maximal to minimal plateau are compared in Figure 2b and referred to as fold damping enhancement. Although damping increases at a faster rate when the gel propagates from the cylinder, the maximum damping enhancement is similar for both configurations utilizing 15 V. Ultimate damping is lower with 5 V, but the subsequent minimal plateau was negligible in comparison to the 15 V groups. This resulted in significantly greater fold enhancement using 5 V. The steep increase in resistance makes 15 V charges efficient for fast adjustments, whereas the slower gelation rate and wider enhancement range of 5 V are appropriate for fine-tuning.

The silk damping fluid requires a significantly lower amount of operating power compared to MR and ER fluids. The disparity in energy usage is potentially magnified over time due to the ability of the silk fluid to maintain damping for longer periods without continuous power. Figure 3 demonstrates the effect of preconditioning the fluid for discrete periods of powered modulation prior to testing the damper unpowered for 10 mechanical stroke cycles over the span of 100 s. Dunnett's multiple comparison post-test was used to compare damping of these strokes using stroke 2 as the control. Stroke 2 was used as the control column in order to account for the initial sloughing of gel which occurs after the first stroke cycle. We see, predictably that there is a significant difference from the first stroke, but that there is no statistically significant difference with any other stroke cycle (p < 0.05). Ultimately, after the operating power is terminated, decay of damping can be expected for any "smart" fluid. However, we demonstrate an unpowered silk fluid damper is capable of functioning without a stark decrease in damping longer in the event of unexpected electrical power loss compared to MR and ER fluids, where damping is lost in milliseconds. Although indefinite powerless operation is neither expected nor our goal; the longer time scale of silk damping decay enables new modulation strategies. In contrast to MR and ER fluids, the silk fluid viscosity does not decrease with field intensity, but responds to it with a decreased rate of gelation. Instead, decreases of electrogel viscosity, which

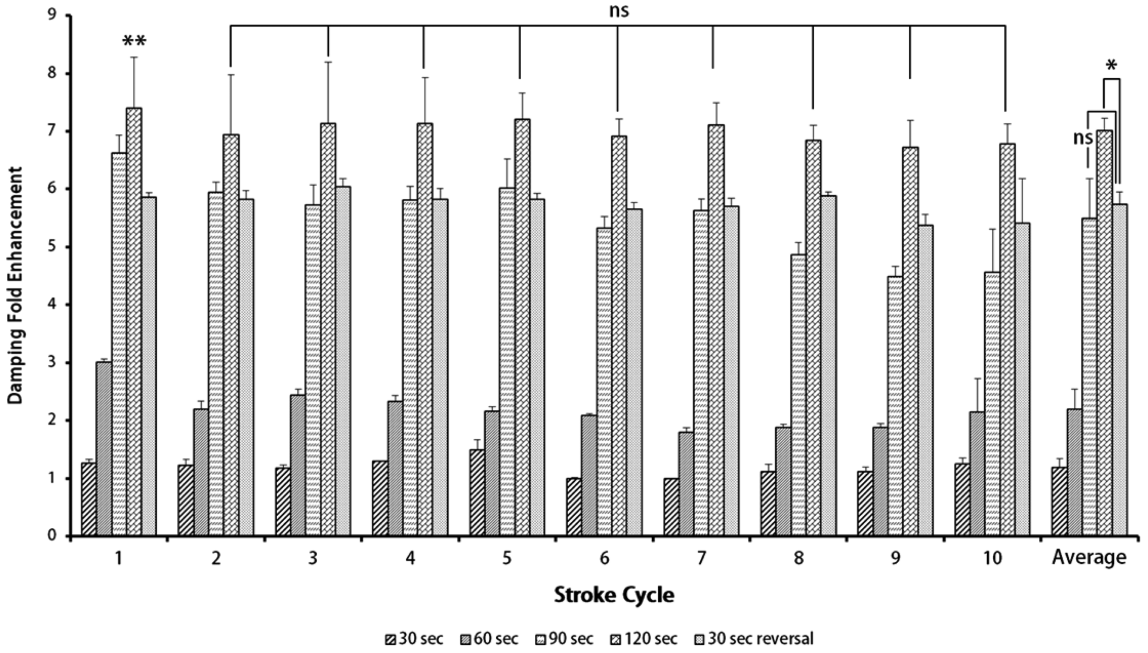

Figure 3. Damping effect was enhanced several-fold with electrogelation time. The 15 V electrical field was disabled after 30, 60, 90, and 120 s thereby halting the gelation process before mechanical testing. The damping effect is shown here persisting throughout ten mechanical testing stroke cycles without applied voltage. Damping of each stroke is compared using stroke 2 as the control (Dunnett's post-test $^{**}p < 0.01$). Variability in damping per each stroke is reported as standard deviation ($n = 40$). After the field was reversed for 30 s the average damping of the strokes ($n = 10$) was similar to 90 s of electrogelation (t test $^{*}p < 0.05$).

can also be modulated with field intensity, require a reversal of the field polarity. The degree of electrogelation is time-dependent; and damping coefficient is progressively enhanced after 30, 60, 90, and 120 s of exposure to a 5 V electric potential at 0.01 A (Figure 3). After 120 s of electrogelation, field reversal for 30 s produces damping results similar to 90 s of electrogelation. The predictable gelation and decay fully facilitates future development of precise programmable control and velocity-driven feedback loops.

In addition to damping, the silk electrogelation results in improved component lubrication and wear reduction. Addition of silk to the device assembly in a low viscosity state allows the solution to easily penetrate between component interfaces. Then, upon field initiation, transformation into a gel state increases resilience of the lubrication layer directly onto the component surfaces. The coefficient of friction is further reduced by as much as 50% as a function of electrogelation time (Table 1). This property leads to striking performance in wear reduction (Table 1). The protective silk coating created using 60 s of electrogelation prevents surface marring by 97% ($n = 3$) and preserves a surface roughness that is not significantly different from the unmarred finish (unpaired t test, $p = 0.8337$).

The electric field can be continuously modulated to automatically alter viscosity in response to changes in loaded weight or rate of compression applied to the damper. Additionally, this feature can be adjusted as desired on-demand in anticipation of needs. The valve assembly can be modified in order to affect the drag thereby altering the damping coefficient. In addition to damping performance due to electrogelation, this system is also compatible with standard damper adjustment mechanisms, such as spring modifications, which enables the possibility of hybrid designs. The combined advantages of the electrogelatable silk fluid allow us to look forward to novel applications. For example, we envision an advanced prosthetic arm design which utilizes the silk fluid to dampen and smooth movements. In the case of unexpected power loss; the silk fluid damper has the potential to provide ample time, at least 100 s, to prevent dropping of critical items. The lower operating current and high biocompatibility of the silk fluid may also improve safety to the user. The silk fluid damper would also facilitate extended powering from small and light portable batteries; whereas MR or ER damping devices would require more cumbersome solutions.

CONCLUSIONS

These results demonstrate the ability of the electrically gelated polymer fluid to provide controlled damping enhancement in the forms of both discrete and/or continuous adjustments. Modulation of the electric field intensity enabled coarse or fine adjustments of damping performance. The biocompatible silk fluid offered improvements in terms of power requirements and powerless damping decay. Electrogelation based dampers can be made in small form factors because they consume less energy and do not require a large number of sophisticated components in order to function. The multifunctional fluid serves to offer a tunable and reversible damping mechanism, penetrating lubrication, and antiwear protection. This also reduces the complexity and potential failure modes of the system in contrast to conventional "smart" damping systems. The silk fluid is nontoxic and biodegradable, which enables the possibility of using this technology in implantable prosthetics or transient biodegradable devices.

ASSOCIATED CONTENT

Supporting Information

Experimental details and additional experimental data. This material is available free of charge via the Internet at http://pubs.acs.org.

AUTHOR INFORMATION

Corresponding Author

*E-mail: david.kaplan@tufts.edu. Phone: (617) 627-3251. Fax: (617) 627-3231.

Author Contributions

The manuscript was written through contributions of all authors. All authors have given approval to the final version of the manuscript.

Funding

The authors thank the National Institutes of Health (P41 EB002520 and 3 P41 EB002520−09S1) and the AFOSR (FA9550−10−1−0172) for financial support.

Notes

The authors declare no competing financial interest.

ACKNOWLEDGMENTS

The authors thank Scott Maccorkle and Denis Dupuis for their machining expertise.

REFERENCES

(1) McIntyre, C.; Yang, H.; Green, P. F. Electrorheology of Suspensions Containing Interfacially Active Constituents. *ACS Appl. Mater. Interfaces* **2013**, *5*, 8925−8931.

(2) Wang, J.; Meng, G. Magnetorheological Fluid Devices: Principles, Characteristics and Applications in Mechanical Engineering. *Proc. Inst. Mech. Eng., Part L: J. Mater. Des. Appl.* **2001**, *215*, 165−174.

(3) Tao, R. Super-Strong Magnetorheological Fluids. *J. Phys.: Condens. Matter* **2001**, *13*, R979−R999.

(4) Ebrahimi, B.; Khamesee, M. B.; Golnaraghi, F. A Novel Eddy Current Damper: Theory and Experiment. *J. Phys. D. Appl. Phys.* **2009**, *42*.

(5) Gong, C.; Hou, L.; Zhu, Y.; Lv, J.; Liu, Y.; Luo, L. In Vitro Constitution of Esophageal Muscle Tissue with Endocyclic and Exolongitudinal Patterns. *ACS Appl. Mater. Interfaces* **2013**, *5*, 6549−6555.

(6) Wu, P.; Liu, Q.; Li, R.; Wang, J.; Zhen, X.; Yue, G.; Wang, H.; Cui, F.; Wu, F.; Yang, M.; et al. Facile Preparation of Paclitaxel Loaded Silk Fibroin Nanoparticles for Enhanced Antitumor Efficacy by Locoregional Drug Delivery. *ACS Appl. Mater. Interfaces* **2013**, *5*, 12638−12645.

(7) Bhattacharjee, M.; Chameettachal, S.; Pahwa, S.; Ray, A. R.; Ghosh, S. Strategies for Replicating Anatomical Cartilaginous Tissue Gradient in Engineered Intervertebral Disc. *ACS Appl. Mater. Interfaces* **2014**, *6*, 183−193.

(8) Yucel, T.; Kojic, N.; Leisk, G. G.; Lo, T. J.; Kaplan, D. L. Non-Equilibrium Silk Fibroin Adhesives. *J. Struct. Biol.* **2010**, *170*, 406−412.

(9) Romero, I. S.; Schurr, M. L.; Lally, J. V.; Kotlik, M. Z.; Murphy, A. R. Enhancing the Interface in Silk−Polypyrrole Composites through Chemical Modification of Silk Fibroin. *ACS Appl. Mater. Interfaces* **2013**, *5*, 553−564.

(10) Xu, S.; Yong, L.; Wu, P. One-Pot, Green, Rapid Synthesis of Flowerlike Gold Nanoparticles/reduced Graphene Oxide Composite with Regenerated Silk Fibroin as Efficient Oxygen Reduction Electrocatalysts. *ACS Appl. Mater. Interfaces* **2013**, *5*, 654−662.

(11) Lu, Q.; Huang, Y.; Li, M.; Zuo, B.; Lu, S.; Wang, J.; Zhu, H.; Kaplan, D. L. Silk Fibroin Electrogelation Mechanisms. *Acta Biomater.* **2011**, *7*, 2394−2400.

(12) Kojic, N.; Panzer, M. J.; Leisk, G. G.; Raja, W. K.; Kojic, M.; Kaplan, D. L. Ion Electrodiffusion Governs Silk Electrogelation. *Soft Matter* **2012**, *8*, 6897−6905.

(13) Yavuz, M.; Tilki, T.; Karabacak, C.; Erol, O.; Ibrahim Unal, H.; Uluturk, M.; Cabuk, M. Electrorheological Behavior of Biodegradable Modified Corn Starch/corn Oil Suspensions. *Carbohydr. Polym.* **2010**, *79*, 318−324.

(14) Lovett, M. L.; Cannizzaro, C.; Daheron, L.; Messmer, B. Silk Fibroin Microtubes for Blood Vessel Engineering. *Biomaterials* **2007**, *28*, 5271−5279.